Orbital and Spin Chains in ZnV_2O_4

S.-H. Lee,[1] D. Louca,[2] H. Ueda,[3] S. Park,[4] T. J. Sato,[3] M. Isobe,[3] Y. Ueda,[3] S. Rosenkranz,[5] P. Zschack,[6] J. Íñiguez,[1] Y. Qiu,[1] and R. Osborn[5]

[1]*NIST Center for Neutron Research, National Institute of Standards and Technology, Gaithersburg, Maryland 20899, USA*
[2]*Department of Physics, University of Virginia, Charlottesville, Virginia 22904, USA*
[3]*Institute for Solid State Physics, University of Tokyo, Kashiwa, Chiba 277-8581, Japan*
[4]*HANARO Center, Korea Atomic Energy Research Institute, Daejeon, Korea*
[5]*Material Science Division, Argonne National Laboratory, Argonne, Illinois 60439, USA*
[6]*Frederick-Seitz Materials Research Lab, University of Illinois at Urbana-Champaign, Illinois 61801, USA*
(Received 29 March 2004; published 7 October 2004)

Our powder inelastic neutron scattering data indicate that ZnV_2O_4 is a system of spin chains that are three-dimensionally tangled in the cubic phase above 50 K due to randomly occupied t_{2g} orbitals of V^{3+} ($3d^2$) ions. Below 50 K in the tetragonal phase, the chains become straight due to antiferro-orbital ordering. This is evidenced by the characteristic wave vector dependence of the magnetic structure factor that changes from symmetric to asymmetric at the cubic-to-tetragonal transition.

DOI: 10.1103/PhysRevLett.93.156407 PACS numbers: 71.70.Ej, 71.27.+a, 75.50.Ee, 78.70.Nx

Cubic spinels AB_2O_4 with magnetic B ions have attracted considerable attention recently in light of geometrical frustration intrinsic to the B-site sublattice of corner-sharing tetrahedra [1]. The long sought zero energy mode of spin fluctuations in the B sublattice [2,3] was found in $ZnCr_2O_4$ [4]. Also in $ZnCr_2O_4$, a spin-Peierls-like transition to relieve frustration was found upon cooling where a tetragonal distortion and a magnetic long-range order occur simultaneously [5]. When the B site is occupied by vanadium ions with orbital degeneracy, complex electronic and magnetic properties emerge. LiV_2O_4, for instance, with monovalent Li ions at the tetrahedral A site and mixed valent $V^{3.5+}$ ions exhibits heavy fermion (HF) behavior at low temperatures with the largest Sommerfeld constant among d-electron systems, $\gamma \approx 0.42$ J/mol K^2 [6]. AV_2O_4 with divalent ions such as Zn [7], Mg [8], Cd [9], at the A site and trivalent V^{3+} ($3d^2$) ions is a Mott insulator [10] that undergoes two separate phase transitions at low temperatures, in contrast to other insulating spinels without orbital degeneracy such as $ZnCr_2O_4$. In this Letter, we show that the orbital degree of freedom plays the central role in the physics of vanadates.

Many theoretical efforts have been made to understand the unusual low temperature behaviors of metallic and insulating vanadates. The macroscopic ground state degeneracy induced by the geometrical frustration intrinsic to the magnetic lattice was attributed to explain the enhancement of the specific heat at low temperatures in LiV_2O_4 [11]. It was also used to explain why the Neél temperature T_N is considerably lower than the Curie-Weiss temperature Θ_{CW} in the insulating vanadates. Spin-lattice coupling mechanisms have been proposed to explain the phase transitions of ZnV_2O_4 [12,13], but fail to explain why the spin and lattice order at different temperatures in the insulating vanadates unlike in $ZnCr_2O_4$. Orbital degeneracy of the vanadium ions was recently considered as well. Fulde *et al.* proposed [14] that due to frustrated charge order or orbital order in LiV_2O_4 ($3d^{1.5}$), one-dimensional chains form, that contribute to the enhancement of the linear term in the specific heat. For insulating AV_2O_4 (A = Zn, Mg, Cd) ($3d^2$), Tsunetsugu and Motome proposed [15] that in the tetragonal ($c < a = b$) phase, among the triply degenerate t_{2g} orbitals, the d_{xy} orbital is favored and is occupied by one electron at every V site. The second electron is in an antiferro-orbital state that can be described by stacking the ab planes along the c axis with alternating d_{yz} and d_{zx} orbitals. This effectively forms straight spin chains on the ab planes. Using a crystal symmetry argument, a ferro-orbital model for the orbital state of the second electron was also proposed [16,17]. To test the validity of these theoretical models, detailed studies of magnetic correlations in the vanadates are necessary to elucidate the interplay between spin, orbital, and lattice degrees of freedom.

The insulating ZnV_2O_4 ($S = 1$) exhibits a sharp drop in the bulk susceptibility, χ, at 50 K [7]. A magnetic long-range order occurs at 40 K with a characteristic wave vector of $\vec{Q} = (110)$ and an ordered moment $\langle M \rangle = g\langle S \rangle = 0.61(3)\ \mu_B/V$ (Fig. 1), in spite of strong magnetic interactions evidenced by the large $|\Theta_{CW}| = JzS(S+1)/3k_B = 998(5)$ K [18,19]. The sharp drop in χ is associated with a structural transition from a high temperature cubic [$a = 8.399\,41(5)$ Å] to a low temperature tetragonal phase [$a_{tet} = 5.948\,07(5)$ Å $\approx a/\sqrt{2}$ and $c_{tet} = 8.37532(1)$ Å] [see Fig. 1(b)]. From our neutron scattering measurements, we find that when the tetragonal distortion occurs, the wave vector (Q) dependence of the inelastic magnetic neutron scattering of the powder sample changes line shape from symmetric centered at $Q_c^{cub} = 1.35(4)$ Å^{-1} to asymmetric peaked at $Q_c^{tet} = 1.10(2)$ Å^{-1}. Quantitative analysis shows that ZnV_2O_4 is a system of three-dimensionally tangled spin chains in the cubic

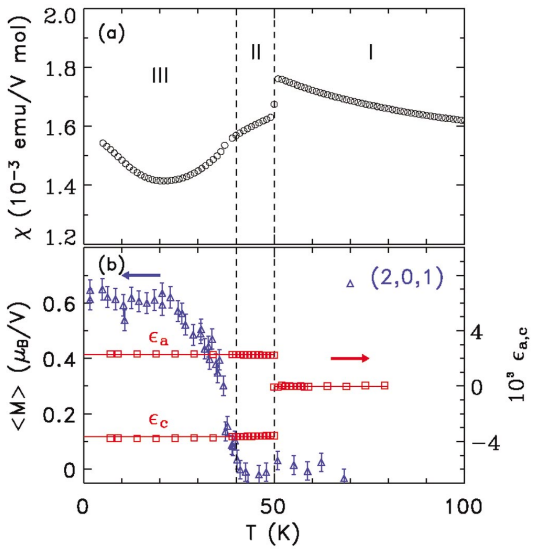

FIG. 1 (color). Temperature dependence of bulk susceptibility, elastic magnetic intensity, and lattice strain. (a) Zero field cooled bulk susceptibility χ. (b) Elastic magnetic intensity (triangles) at $Q = 1.67$ Å^{-1} that corresponds to the magnetic (2, 0, 1) reflection with a saturation moment of $\langle M\rangle = g\langle S\rangle = 0.61(3)\mu_B$ per V ion (g-gyromagnetic ratio), and lattice strain (squares) along a and c measured by synchrotron x-ray diffraction on a single crystal with dimensions of 10^{-3} mm^3 (6 μg). The x-ray measurements were carried out at the 33BM-C beam line at the Advanced Photon Source of Argonne National Laboratory.

phase. On the other hand, in the tetragonal phase ZnV_2O_4 becomes an excellent model system for one-dimensional spin chains. This favors the antiferro-orbital model that yields straight chains in the *ab* planes with *weak* interchain interactions. We argue that our findings provide a unified picture of the physics of vanadates, both insulating and metallic.

A 30 g polycrystalline sample of ZnV_2O_4 was used for the neutron scattering experiments. The elastic measurements were performed using the cold neutron triple-axis spectrometer SPINS at the National Institute of Standards and Technology Center for Neutron Research with a fixed incident and scattered neutron energy of $E_i = 3.1$ meV. The inelastic measurements were carried out on the time-of-flight spectrometer LRMECS with a detector arrangement covering scattering angles from 7.5° to 118°, at the Intense Pulsed Neutron Source of Argonne National Laboratory and with an incident energy, $E_i = 30$ meV.

Figure 2 is an overview of the inelastic neutron scattering data in the form of color images of intensity, $I(Q, \hbar\omega)$, as a function of Q and energy transfer, $\hbar\omega$, in three different phases. Data were collected up to $Q = 6.5$ Å^{-1} but shown only up to 2.5 Å^{-1} in Fig. 2. In the cubic phase I ($T > 50$ K), strong low energy magnetic excitations are present in the form of a broad peak centered at $Q_c^{\rm cub} = 1.35(4)$ Å^{-1} shown in Fig. 2(a). In phase II (40 K $< T <$ 50 K) with the tetragonal distortion but no magnetic long-range order, a similar broad peak is present at low energies. However, the broad peak is strikingly asymmetric in Q and shifts to a lower characteristic wave vector, $Q_c^{\rm tet} = 1.10(2)$ Å^{-1} [Fig. 2(b)]. In the tetragonal Néel phase III ($T < 40$ K), the asymmetry of the broad feature in Q remains but spectral weight in the inelastic scattering cross section shifts in energy to have a broad feature peaked at around 11 meV [Fig. 2(c)]. The change from symmetric to asymmetric Q dependence of the spin excitations between 100 and 45 K indicates that there is a crossover in the nature of the magnetic correlations from three dimensions to a lower dimension [20] between phases I and II.

The energy integrated inelastic magnetic neutron scattering intensity as a function of Q is shown at several temperatures in Fig. 3. The phonon contribution was determined first at 100 K by fitting the data to a Q^2 term for $Q > 5$ Å^{-1}, was multiplied by the thermal population factor to estimate the contribution at lower temperatures, and was subtracted from the data. In phase I of the 60 and 100 K data, the broad peak centered around 1.35(4) Å^{-1} can be attributed to cooperative paramagnetic spin fluctuations induced by geometrical frustration intrinsic to the magnetic lattice. Since magnetism in both $ZnCr_2O_4$ ($3d^3$) and ZnV_2O_4 ($3d^2$) involves t_{2g} electrons, one may think that their magnetic fluctuations should have the same fundamental spin degrees of freedom. If that is the case, antiferromagnetic hexagonal spin loops

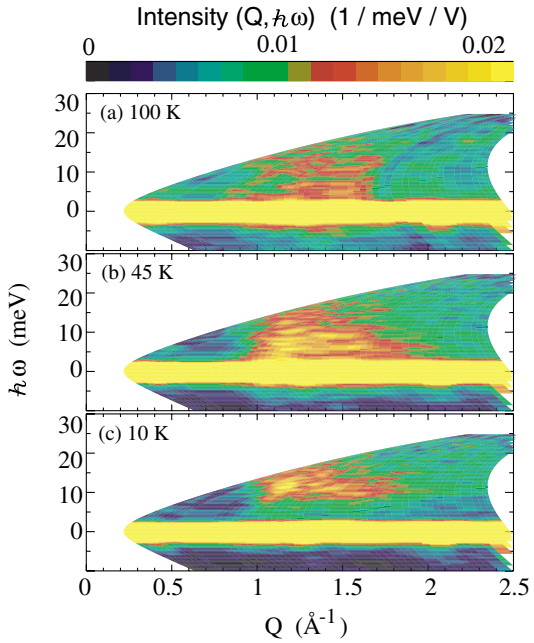

FIG. 2 (color). Neutron scattering intensity as a function of energy ($\hbar\omega$) and wave vector (Q) transfer obtained from a powder sample of ZnV_2O_4 at three different phases. (a) At 100 K, in the cubic and cooperative paramagnetic phase. (b) At 45 K, in the tetragonal phase without magnetic long-range order. (c) At 10 K, in the tetragonal and Néel phase.

are the fundamental spin degrees of freedom and will produce magnetic neutron scattering with the characteristic wave vector of $Q_c^{\mathrm{hex}} = 1.5$ Å^{-1} [4,5,13]. The Q_c^{hex}, however, is inconsistent with the observed peak position [$Q_c^{\mathrm{cub}} = 1.35(4)$ Å^{-1}], which tells that dynamic spin correlations in ZnV_2O_4 are different in nature than those in $ZnCr_2O_4$. In order to explain our data, we considered a model similar to the one proposed in Refs. [14,21] that takes the orbital degeneracy of $V^{3+}(3d^2)$ ions into account. Since in the cubic phase the three t_{2g} orbitals, d_{xy}, d_{yz}, and d_{zx}, are equivalent, we assume that at each V site their occupancy fluctuates with time with an equal probability of 1/3. At an instant time, two out of the three orbitals are randomly occupied at all V^{3+} sites. We considered a model with $12 \times 12 \times 12$ cubic unit cell with such randomly occupied t_{2g} orbitals. Figure 4(a) shows a schematic representation of one such unit cell. We subsequently consider all possible magnetic interactions due to direct overlap of the orbitals to obtain the effective fluctuating spin objects. Shown as sky blue rods in Fig. 4(a), the resulting fluctuating spin objects form three-dimensionally tangled antiferromagnetic spin chains. The solid lines in Figs. 3(a) and 3(b) are the powder-averaged resulting structure factor squared from this model that reproduces the data well including the characteristic wave vector Q_c^{cub}.

In the tetragonal phases II and III, spin fluctuations change dramatically, with a sharp increase at low Q and a long tail at high Q. It is clear that the asymmetric line shape cannot be explained by the two models discussed above for the cubic phase. Instead, as shown by the solid lines in Figs. 3(c) and 3(d) the asymmetric line shape can be directly fit to the dynamic structure factor based on the single mode approximation [22],

$$S(\vec{Q}, \omega) \propto |F(Q)|^2 \frac{1 - \cos(\vec{Q} \cdot \vec{d})}{\hbar\omega_{\vec{Q}}} \delta(\omega - \omega_{\vec{Q}}), \quad (1)$$

where $\vec{d}$ is the intrachain spacing for a one-dimensional (1D) spin chain. Here $F(Q)$ is the magnetic form factor for the V^{3+} and the spin wave dispersion relation is $\hbar\omega_{\vec{Q}} = \sqrt{\Delta^2 + v^2 \sin^2(\vec{Q} \cdot \vec{d})}$ where Δ is a spin gap and v is the spin wave velocity. The optimal intrachain spacing, d, obtained from the fitting is consistent with the distance between nearest neighboring V^{3+} ions: $d = \pi/Q_c^{\mathrm{tet}} = 2.97\,\text{Å} = a_{\mathrm{tet}}/2$. The excellent agreement between the 1D chain model and data indicates that below the tetragonal transition, ZnV_2O_4 is a system of one-dimensional antiferromagnetic spin chains. This one dimensionality of the magnetic interactions can be understood if two orbitals per V ion are occupied in a striated form along the c axis, as shown in Fig. 4(b). One electron from every V ion resides in the d_{xy} orbital while the occupancy of the second electron can be described by stacking the ab planes with alternating d_{yz} and d_{zx} orbitals along the c axis [15]. The direct overlap of neighboring t_{2g} orbitals occurs only between d_{xy} orbitals, yielding orbital chains and thereby one-dimensional antiferromagnetic spin

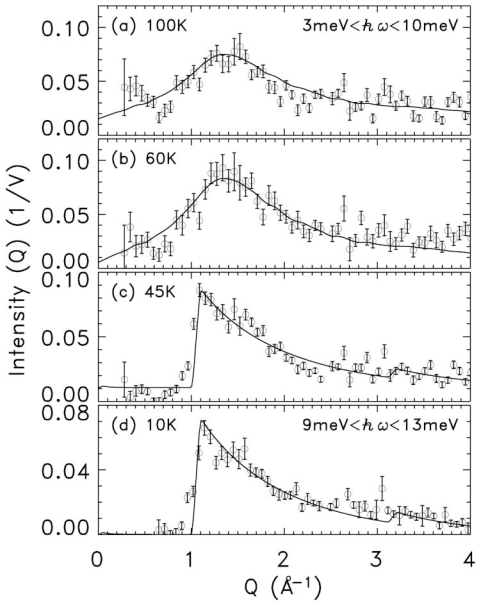

FIG. 3. Q dependence of inelastic magnetic neutron scattering intensity obtained by integrating the data shown in Fig. 1 over the range of energy that includes most of the excited spectral weight: (a) at 100, (b) 60, (c) 45, and (d) 10 K. The energy integration range is 3 meV $< \hbar\omega <$ 10 meV for (a), (b), and (c) and 9 meV $< \hbar\omega <$ 13 meV for (d). Lines are fits to the models explained in the text.

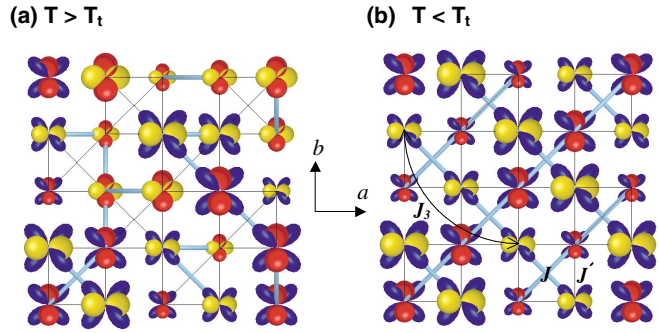

FIG. 4 (color). (a),(b) Illustrations of the orbital states of ZnV_2O_4 in one cubic unit cell. Balloons represent the t_{2g} orbitals of the $V^{3+}(3d^2)$ ions: d_{xy} (blue), d_{yz} (red), and d_{zx} (yellow) orbitals located at the vanadium site. The four different sizes of the balloons represent four different ab planes with different z coordinates. (a) The cubic phase above 50 K. The three orbitals are randomly distributed. The blue rods connect possible dynamic magnetic interactions at a snap shot due to direct overlap of the neighboring orbitals. (b) Antiferro-orbital model for the tetragonal phase. J, J', and J_3 represent coupling constants for the nearest neighbor intrachain, the nearest neighbor interchain (interplane), and the second nearest neighbor intrachain interactions, respectively. In this model, J' is negligible because d_{yz} and d_{zx} orbitals do not overlap.

chains in the ab planes. The V^{3+} magnetic moments do not order even in the orbitally ordered state because of the one dimensionality of the magnetic interactions until weak further nearest neighbor interactions set in [23]. Ferro-orbital ordering where the second electron of every V^{3+} ion resides on the $(d_{yz} \pm id_{zx})/\sqrt{2}$ orbitals, has also been proposed [17]. However, in this model the orbitals of the neighboring second electrons do overlap directly with each other leading to stronger interchain interactions by at least $|J'| \sim 0.25J$ [16] and this would generate a much less asymmetric line shape in $S(Q)$ than observed [24].

Until now, ZnV_2O_4 was considered to be a geometrically frustrated magnet similarly to $ZnCr_2O_4$ because the magnetic V^{3+} ions form a lattice of corner-sharing tetrahedra in the crystal structure. However, our results show that due to the orbital degree of freedom ZnV_2O_4 should be considered as a system of spin chains, instead. In the cubic phase, the random occupancy of the t_{2g} orbitals renders a system of three-dimensionally tangled spin chains. In the tetragonal phase ($c < a = b$), on the other hand, antiferro-orbital ordering occurs that yields a system of weakly interacting straight spin chains in the ab planes. This picture can also be used to explain the phase transitions observed in other insulating vanadates, AV_2O_4 ($A =$ Mg and Cd). The tetragonal transition occurs at $T_t = 65$ and 97 K whereas the Néel ordering occurs at $T_N = 42$ and 35 K for Mg and Cd, respectively. T_t is determined by the balance among thermal energy, the energy gain from orbital ordering and the energy cost for the lattice distortion. When the A site is occupied by a larger ion, e.g., Cd^{2+} instead of Zn^{2+} or Mg^{2+}, the lattice becomes softer and the tetragonal distortion occurs at a higher temperature. T_N, on the other hand, is determined by the strength of interchain coupling, and therefore it is lower for Cd^{2+} where the interchain coupling is weaker due to the larger distance between V ions.

These results may have significant implications on the physics of metallic LiV_2O_4 as well. Our finding that the cubic phase of ZnV_2O_4 consists of three-dimensionally tangled fluctuating spin chains suggests that the one dimensionality of the magnetic fluctuations may play an important role in LiV_2O_4 that remains cubic down to 20 mK [26]. It was previously found that LiV_2O_4 exhibits strong antiferromagnetic spin fluctuations when the system enters the heavy fermionic phase at low temperatures [27]. If we consider that the orbital degree of freedom is important in this system as in the cubic phase of ZnV_2O_4, then the formation of three-dimensionally tangled fluctuating orbital chains may also occur in LiV_2O_4. The metallic character of LiV_2O_4 may produce a spin-density wave along the orbital chains that is responsible for the strong antiferromagnetic spin fluctuations and the enhancement of the low energy density of states at low temperatures.

We thank D. I. Khomskii, C. Broholm, and J. B. Goodenough for valuable discussions. This work was partially supported by the NSF under Agreement No. DMR-9986442 and the DOE under Contracts No. DE-FG02-01ER45927, No. W-31-109-ENG-38, No. DE-FG02-91ER45439, and No. DE-AC05-00OR22725.

[1] A. P. Ramirez, *Handbook on Magnetic Materials*, edited by K. J. H. Busch (Elsevier Science, Amsterdam, 2001), Vol. 13, p. 423
[2] R. Moessner and J. T. Chalker, Phys. Rev. Lett. **80**, 2929 (1998); Phys. Rev. B **58**, 12 049 (1998).
[3] B. Canals and C. Lacroix, Phys. Rev. Lett. **80**, 2933 (1998).
[4] S.-H. Lee *et al.*, Nature (London) **418**, 856 (2002).
[5] S.-H. Lee *et al.*, Phys. Rev. Lett. **84**, 3718 (2000).
[6] S. Kondo *et al.*, Phys. Rev. Lett. **78**, 3729 (1997); Phys. Rev. B **59**, 2609 (1999).
[7] Y. Ueda *et al.*, J. Phys. Soc. Jpn. **66**, 778 (1997).
[8] H. Mamiya *et al.*, J. Appl. Phys. **81**, 5289 (1997).
[9] N. Nishiguchi and M. Onoda, J. Phys. Condens. Matter **14**, L551 (2002); M. Onoda and J. Hasegawa, J. Phys. Condens. Matter **15**, L95 (2003).
[10] A. Fujimori *et al.*, Phys. Rev. B **38**, 7889 (1988).
[11] V. Eyert *et al.*, Europhys. Lett. **46**, 762 (1999).
[12] Y. Yamashita and K. Ueda, Phys. Rev. Lett. **85**, 4960 (2000).
[13] O. Tchernyshyov *et al.*, Phys. Rev. Lett. **88**, 067203 (2002); Phys. Rev. B **68**, 144422 (2003).
[14] P. Fulde *et al.*, Europhys. Lett. **54**, 779 (2001).
[15] H. Tsunetsugu and Y. Motome, Phys. Rev. B **68**, 060405 (2003).
[16] D. I. Khomskii (private communication).
[17] O. Tchernyshyov, cond-mat/0401203 [Phys. Rev. Lett. (to be published)].
[18] S. Nizioł, Phys. Status Solidi A **18**, K11 (1973).
[19] M. Reehuis *et al.*, Eur. Phys. J. B **35**, 311 (2003).
[20] B. E. Warren, Phys. Rev. **59**, 693 (1941).
[21] S. Fujimoto, Phys. Rev. B **65**, 155108 (2002).
[22] G. Xu *et al.*, Phys. Rev. B **54**, 6827(R) (1996).
[23] Y. Motome and H. Tsunetsugu, cond-mat/0406039 [Phys. Rev. B (to be published)]. This Monte Carlo study on a Hubbard Hamiltonian shows that the antiferro-orbital model with J, $|J_3/J| \sim 0.02$, and $J' = 0$ can explain the two phase transitions in ZnV_2O_4.
[24] $ZnCr_2O_4$ that realizes a $J' \simeq J$ in its cubic and tetragonal phases exhibits a symmetric powder Q line shape in both phases due to the three-dimensional hexagonal antiferromagnetic fluctuations [5,25]. For the ferro-orbital case of $J'/J \sim 0.25$, we expect the powder Q line shape to be less symmetric than the powder-averaged structure factor for the 3D hexagonal fluctuations but less asymmetric than the structure factor of the 1D spin chain.
[25] W. Ratcliff *et al.*, Phys. Rev. B **65**, 220406(R) (2002).
[26] A. Koda *et al.*, Phys. Rev. B **69**, 012402 (2004).
[27] S.-H. Lee *et al.*, Phys. Rev. Lett. **86**, 5554 (2001).